JOURNAL OF ADVANCED MECHANICAL ENGINEERING APPLICATIONS
e-ISSN: 2716-6201

JAMEA

Vol. 6 No. 1 (2025) 80-93
https://publisher.uthm.edu.my/ojs/index.php/jamea

Analysis of MgFeCu-Layered Double Hydroxides with Different Interlamellar Anions for Efficient Removal of Dye in Wastewater Treatment

Muhammad Syaza Mohd Sahabudin[1], Norrizal Mustaffa[2]*, Nurasyikin Misdan[2]

[1] *Faculty of Mechanical and Manufacturing Engineering, Universiti Tun Hussein Onn Malaysia, Parit Raja, 86400, Johor, MALAYSIA*
[2] *Department of Mechanical Engineering Technology, Faculty of Mechanical and Manufacturing Engineering, Universiti Tun Hussein Onn Malaysia, Parit Raja, 86400, Johor, MALAYSIA*

*Corresponding Author: norrizal@uthm.edu.my
DOI: ://doi.org/10.30880/jamea.2025.06.01.007

Article Info

Received: 4 March 2025
Accepted: 21 April 2025
Available online: 30 June 2025

Keywords

Adsorption, layered double hydroxides, wastewater treatment, XRD, kinetic adsoption model

Abstract

Synthetic dyes, widely used in industries like textiles, leather, and paper, pose a significant global concern for water pollution due to their resistance to conventional wastewater treatment, causing toxic, carcinogenic, and mutagenic effects, endangering aquatic life and disrupting natural processes like photosynthesis. The study analyzes the adsorption of as-prepared MgFeCu- Layered Double Hydroxides (LDH) with varied interlamellar anions (CO_3^{2-}, SO_4^{2-}, NO_3^-) on dye wastewater, utilizing advanced techniques like Scanning Electron Microscopy (SEM) and X-ray Diffraction (XRD) to identify LDH morphology and crystal structure, elucidating dye removal mechanisms. The methods and materials used in this study include synthesizing MgFeCu-Layered Double Hydroxides with various interlamellar anions using co-precipitation and involved weighing 50 mg of LDH and 30 ml of dye solution, equilibrating samples, and analyzing UV analysis and storage to determine the amount of adsorbed MO in the supernatants, followed by adsorption kinetic studies to evaluate the efficiency and mechanisms of dye removal from wastewater, focusing on pseudo-second-order kinetic models to determine the dominant adsorption processes. MgFeCu-SO_4 LDH removes dyes from wastewater in 150 minutes using a second-order process, providing a quick, cost-effective, and environmentally friendly solution. The findings provide important insights into the development of novel materials to address the persistent problem of synthetic dye contamination in aquatic systems, highlight the potential of LDH materials for wastewater treatment, as they offer a scalable approach to dye removal via tailored chemical and structural properties.

1. Introduction

Industrial activities have increased the release of synthetic dyes into aquatic environments, posing serious threats to human health and ecosystems. These dyes, which are used in industries such as paper, plastic, leather, and textiles, are resistant to conventional wastewater treatment methods due to their complex molecular structures. Many are toxic, carcinogenic, and mutagenic, reducing light penetration and impairing

photosynthesis in aquatic environments. Layered Double Hydroxides (LDHs), particularly MgFeCu-LDHs, have high potential for environmental remediation due to their large surface area and ion exchange capabilities. This study investigates the effectiveness of MgFeCu-LDHs in dye removal by examining adsorption kinetics, isotherms, and thermodynamics, as well as assessing their regeneration potential. The study's goal is to create a sustainable and efficient solution for treating dye-contaminated wastewater by optimizing operational parameters [1].

Dyes are used in industries to keep sunlight and oxygen from entering water bodies. Liquid hydrogen peroxide (LDH) has excellent adsorption performance in the treatment of printing and dyeing wastewater due to its anion exchange capacity, memory effect, and large specific surface area. Dye adsorption mechanisms are classified into three types: electrostatic attraction, ion exchange, and complexation. A series of functional LDH-based materials have been synthesized to remove dye from water [2]. LDHs are extremely effective at removing contaminants because of their large surface area, high anion exchange capacity, and flexible interlayer region. They have been used to remove a variety of dyes, including cationic, anionic, and non-ionic types. Temperature, concentration, and LDH functional groups all have a significant influence on dye adsorption capacity [3].

Since the discovery of brucite, LDHs have received a lot of attention. Because natural LDHs are scarce and unrefined, synthetic LDHs with metal type and interlayer space tunability are in high demand for a wide range of applications. The type and quantity of metal elements present in an LDH determines whether it is binary, ternary, or tetradentate. A binary LDH has two cations, a ternary LDH has three, and a quaternary LDH has four [4]. Because of the carefully controlled chemical composition of the lamellar layers and interlayer composition, LDHs have a unique supramolecular nanometric structure that can disperse active sites on an atomic scale and facilitate morphological manipulation. As a result of their versatile chemical makeup and nanostructure, LDHs show promise as adsorbents against a wide range of pollutants. The space between layers, the large surface area capable of adsorbing bioactive substances, which are primarily determined by the synthesis conditions, and the chemical compositions of LDHs based on the metals used are their most appealing features [5].

Adsorption is the process by which an adsorbate, an ion or molecule found in a gaseous or liquid bulk, adheres to the surface of an adsorbent, which is typically a solid. Adsorbate does not permeate the adsorbent's structure; rather, it affects the material's surface; in this case, the process is referred to as absorption. Desorption is the opposite process, which is the dropping of a molecule from a solid surface. The LDH-EDTA-AM composite was used to test dye removal from combined contaminants. The primary adsorption mechanisms are electrostatic attraction, surface complexation, and anion exchange. The LDH/MOF composite improved adsorption of reactive dye Orange II, with a maximum adsorption amount of 1173 mg/g. Nanocomposite beads made of chitosan, tannic acid, LDH, and mixed metal oxides effectively removed three reactive dyes with adsorption capacities ranging from 257 to 483 mg g−1[2]. This study attempts to close this gap by methodically examining how well MgFeCu-LDHs remove dyes from wastewater. To comprehend the mechanisms underlying the interactions between the dyes and the LDH material, the study will look into the adsorption kinetics, isotherms, and thermodynamics [6].

The design and application of a suitable adsorbent necessitates a number of attributes, including low production costs, thermal, mechanical, and chemical stabilities, desirable physicochemical properties like elevated textural properties and high surface functional group availability, high efficiency and adsorption capacity, rapid kinetics, and regeneration/reuse potential. Some of the aforementioned properties can only be verified when the material is applied in a particular process because they depend on the adsorbate's characteristics and operating conditions [5].

2. Methodology

2.1 Materials Preparation

For the studies, an industrial dye wastewater, methyl orange (MO) used as the sample. The chemicals used in this experiment include Fe(NO3)3.9H2O, Mg(NO3)2.6H2O, Cu(NO3)2.3H2O, Na2CO3, Na2SO4, NaOH, and NaNO.

2.2 Synthesis of LDH

In the layered double hydroxide (LDH) synthesis process, the constant pH method entails regulating the pH during co-precipitation, which precipitates the LDH material by adding metal solutions to an alkaline solution, usually NaOH. The formation of the LDH structure and its characteristics are impacted by the accurate pH control made possible by this technique [16].

MgFeCu-CO_3 synthesized using the Constant-pH Method. To adjust the pH to 10.0, 500 mL of H_2O was heated at 40°C and a solution of 1.0 M Na_2CO_3 and 2.0 M NaOH was added. A mixed metal nitrate solution with a Cu2+/Mg2+/Fe3+ molar ratio of 0.011 mol Cu(II), 0.109 mol Mg(II), and 0.040 mol Fe(III), as well as the mixed base solution, were then added to the reaction vessel at rates that kept the reaction pH at 10.0. Once the mixed base solution had been consumed, 2.0 M NaOH was added to maintain the pH of 10.0 for the remainder of the

precipitation reaction. The reaction mixture was vigorously stirred for 4 hours at 40°C, then aged for 40 hours at 70°C, with good stirring. Following the digestion period, the product suspension was cooled to room temperature and centrifuged. The resulting white product was then washed to remove carbonate ions (as determined by the $AgNO_3$ test) by repeatedly forming a slurry in deionized water and centrifuging. The final products were air-dried on a glass plate.

MgFeCu-SO_4 synthesized using the Constant-pH Method. To adjust the pH to 10.0, add several drops of a solution made by mixing equal volumes of 1.0 M Na_2SO_4 and 2.0 M NaOH to 500 mL of water heated at 40°C. A mixed metal nitrate solution with a Cu2+/Mg2+/Fe3+ molar ratio of 0.011 mol Cu(II), 0.109 mol Mg(II), and 0.040 mol Fe(III), as well as the mixed base solution, were then added to the reaction vessel at rates that kept the reaction pH at 10.0. Once the mixed base solution had been consumed, 2.0 M NaOH was added to maintain the pH of 10.0 for the remainder of the precipitation reaction. The reaction mixture was vigorously stirred for 4 hours at 40°C, then aged for 40 hours at 70°C, with good stirring. Following the digestion period, the product suspension was cooled to room temperature and centrifuged. The resulting white product was then washed to remove carbonate ions (as determined by the $AgNO_3$ test) by repeatedly forming a slurry in deionized water and centrifuging. The final products were air-dried on a glass plate.

MgFeCu-NO_3 synthesized using the Constant-pH method. To adjust the pH to 10.0, 500 mL of H_2O was heated at 40°C and a solution of 1.0 M $NaNO_3$ and 2.0 M NaOH was added. A mixed metal nitrate solution with a Cu2+/Mg2+/Fe3+ molar ratio of 0.011 mol Cu(II), 0.109 mol Mg(II), and 0.040 mol Fe(III), as well as the mixed base solution, were then added to the reaction vessel at rates that kept the reaction pH at 10.0. Once the mixed base solution had been consumed, 2.0 M NaOH was added to maintain the pH of 10.0 for the remainder of the precipitation reaction. The reaction mixture was vigorously stirred for 4 hours at 40°C, then aged for 40 hours at 70°C, with good stirring. Following the digestion period, the product suspension was cooled to room temperature and centrifuged. The resulting white product was then washed to remove carbonate ions (as determined by the $AgNO_3$ test) by repeatedly forming a slurry in deionized water and centrifuging. The final products were air-dried on a glass plate. Fig. 1 shows the LDH after drying in powder.

(a) **(b)** **(c)**

Fig. 1 *LDH after drying in powder, (a) MgFeCu- SO_4; (b) MgFeCu-NO_3; and (c) MgFeCu- CO_3*

2.3 Preparation of Dye Solution

Dyes are used in industries to keep sunlight and oxygen from going into water bodies. The anion exchange capacity, memory effect, and large specific surface area of liquid hydrogen peroxide (LDH) make it an excellent adsorbent for treating wastewater from printing and dyeing. Ion exchange, complexation, and electrostatic attraction are the three categories of dye adsorption mechanisms. To extract dye from water, a number of useful LDH-based materials have been created [2].

100mg of Methylene Orange (MO) was dissolved in 1000ml of distilled water to make a 100 mgl-1 stock solution. The experimental solution was created by diluting the stock solution to a concentration of 20-80 mgl-1 with distilled water. The concentration of MO was measured at 648 nm using a Shimadzu UV 1600 spectrophotometer [7]. By following past experiment with some modification, this experiment use 1000ml of distilled water was used to dissolve 100mg of MO to create an experiment solution with a concentration of 100 mgl-1, which was then separated into 9 glass containers containing 30ml each of MgFeCu-LDH as shown in Fig. 2. The concentration of MO was measured at 464 nm using a Shimadzu UV 1600 spectrophotometer.

Fig. 2 *Methyl Orange 30ml concentration of 100 mgl^{-1}*

2.4 Batch Adsorption Procedure

The experiments employed a 25 mg dose of LDH in 20ml of dye solution at the desired contact time and initial MO concentration. Each 0.025g powdered sample was collected and weighed using an electronic weighing balance (as shown in Fig 3); the weighed samples were placed in clean beakers. 20ml of dye solutions with standard concentrations were prepared from the stock solution and added to the weighed mass of LDH. The samples were agitated (shaken) for 5, 10, 15, 20, and 25 minutes to equilibrate them. The sample suspensions were centrifuged for 5 minutes, decanted, and the supernatants were saved for dye time measurements. Time differential studies were conducted with initial concentrations of 20, 40, 60, and 80 mg/L, and the supernatants were stored and used for UV analysis (UV 1600, Shimadzu) [7].

By following past experiment with some modification, this experiment uses 50 mg of LDH with 30ml of dye solution at the desired contact time and initial MO concentration. Each 0.050g powdered sample was collected and weighed using an electronic weighing balance; the weighed samples were then placed on filter paper. 30ml of dye solutions (MO) at 100mgl-1 concentrations were prepared and mixed with the weighed mass of LDH. The samples were equilibrated by shaking the beaker, and they were collected at minutes 5, 10, 20, 30, 50, 70, 90, 120, and 150 without removing the precipitate of LDH particles below. Fig. 4 shows the Methyl Orange colour after putting $MgFeCu.CO_3$. For time differential studies, initial concentrations of 100 mg/L were used, and the supernatants were stored and analysed using UV. The amount of adsorbed MO was determined by quantifying the un-adsorbed moiety in the supernatants using visible light spectroscopy (UV-1800, Shimadzu, Kyoto, Japan) at λ max of 464 nm as shown in Fig. 5.

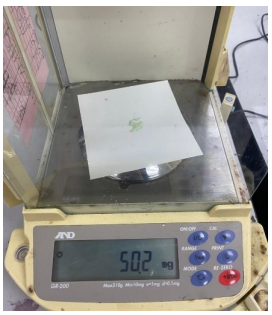

Fig. 3 *50 mg MgFeCu-CO_3 powder is weighed using analytical balance*

Fig. 4 *Methyl orange colour after putting $MgFeCu.CO_3$*

Fig. 5 *UV 1800 Shimadzu spectrophotometer*

2.5 Characterization of LDH

Using A JEOL 7500 F, field emission scanning electron microscope (FESEM), surface structures and morphologies of $MgFeCu.CO_3$, $MgFeCu.NO_3$, and $MgFeCu.SO_4$ are analysed methodically. To reduce charging effects during imaging, the samples must first be properly prepared by drying to remove any remaining moisture, then mounting them on aluminium stubs with conductive carbon tape or paste and applying a thin conductive layer (such as gold or platinum). FESEM can show intricate structural details at high magnifications, ranging from 1,000× for an overview to 50,000 with an acceleration voltage of 1-5 kV. Backscattered electron (BSE) imaging can provide compositional contrast, but secondary electron (SE) imaging is preferred for surface morphology.

X-Ray Diffraction (XRD)(as shown in Fig. 6) is a critical technique for determining the crystalline structure of materials such as Layered Double Hydroxides. It provides information about the phase purity, crystallinity, and interlayer spacing of LDHs, which is critical for understanding their adsorption properties. The interlayer region in LDHs contains a variety of anions, and their arrangement influences the material's structural and functional characteristics. LDH XRD patterns typically show sharp and intense basal reflections, indicating a layered structure, as well as weaker non-basal peaks. Changes in peak positions, intensities, or patterns may indicate anion intercalation or dye adsorption. By analysing the XRD results, researchers can confirm the successful synthesis of LDHs and assess their structural stability during adsorption.

Fig. 6 *XRD (Bruker D8 Advance Eco)*

3. Results and Discussion

3.1 LDH Properties Analysis

The topic focusses on analysing the catalyst's physical and chemical properties using advanced techniques for analysis, such as XRD to analyse crystalline structure, and Scanning Electron Microscopy (SEM) to examine surface morphology as shown in Fig. 7.

3.1.1 Result of SEM

$MgFeCu.CO_3$ typically has rhombohedral crystals or spherical aggregates, while $MgFeCu.NO_3$ may form rod- or needle-shaped particles due to nitrate crystallization properties. $MgFeCu.SO_4$ may have prismatic or plate-like structures, as sulfates often crystallize in different morphologies. Energy-dispersive X-ray spectroscopy (EDS), which maps the distribution of Mg, Fe, Cu, C, O, N, and S to confirm the presence of carbonate, nitrate, and sulfate groups in each compound, can help with morphological analysis by confirming elemental composition [8].

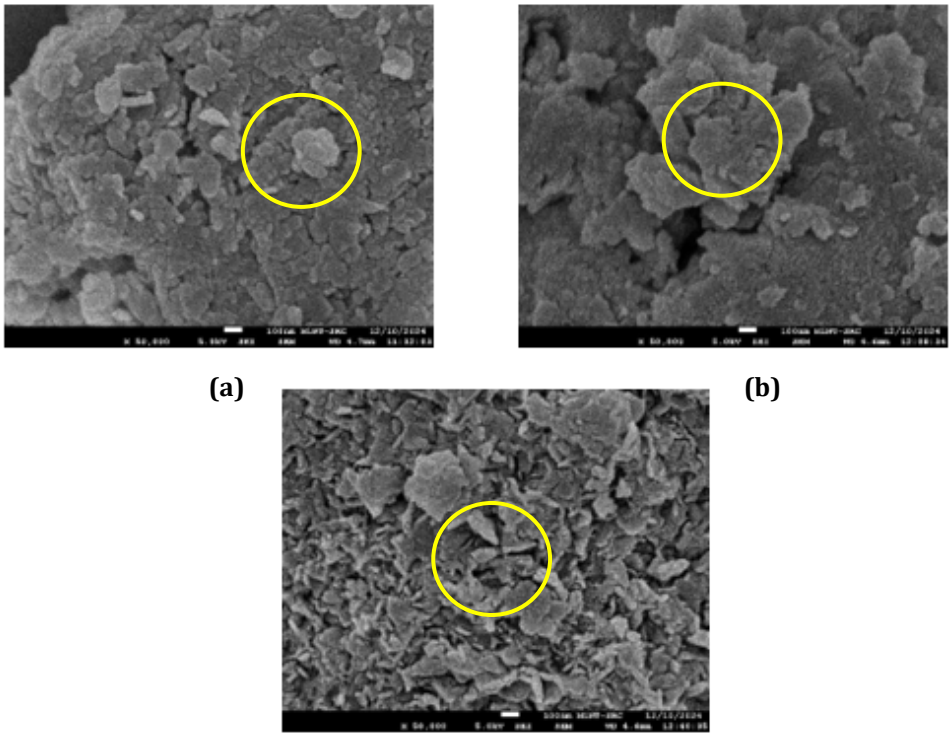

Fig. 7 *SEM images at different magnifications of (a) MgFeCu-CO_3 with spherical aggregates shape; (b) MgFeCu-NO_3 rod-shaped particles; and (c) MgFeCu-SO_4 with prismatic structures*

In terms of morphology, MgFeCu.CO_3 is expected to display carbonate-like structures like spherical aggregates or rhombohedral crystals. The carbonate groups' inherent crystal lattice, which frequently encourages symmetrical growth, is what causes these formations. Rapid precipitation during synthesis may have produced the spherical aggregates, which resulted in uniform, isotropic growth. MgFeCu.CO_3 surface textures may also be a sign of changes in the growth environment, such as shifts in pH or temperature during crystallization [8].

Because of the anisotropic nature of nitrate crystallization, needle-like or rod-shaped particles are anticipated in the case of MgFeCu.NO_3. The planar molecular structure of nitrate anions tends to promote elongated crystal growth along specific crystallographic axes. Precursor concentration and crystallization rate are two examples of synthesis conditions that are frequently reflected in the final morphology. Additionally, these elongated structures might show aggregated clusters or porosity, which could be signs of specific metal-ion interactions or incomplete crystallization [8].

In contrast, MgFeCu.SO_4 is likely to form prismatic or plate-like particles. Because sulfates can create strong ionic bonds with metal cations, they frequently crystallize in distinct shapes. Prismatic structures indicate controlled growth along several axes, which is frequently made possible by synthesis methods such as hydrothermal methods or slow crystallization processes. If the growth environment contained impurities or fluctuating conditions, the surface texture of these crystals may exhibit rough surfaces or faceting, which is a sign of high crystallinity [8].

3.1.2 Result of XRD

Each compound's diffractogram displays unique peak patterns that match its distinct crystalline phases as shown in Fig. 8, Fig. 9 and Fig 10. The XRD data for MgFeCu.CO_3 shows distinct peaks at particular 2-theta values, indicating a high degree of crystallinity. A stable crystal structure, which is necessary for efficient adsorption properties, is indicated by the sharpness of the peaks. When compared to MgFeCu.CO_3, the XRD patterns for MgFeCu.NO_3 exhibit differences in peak positions and intensities. These variations could point to impurities present during synthesis or modifications in the crystal structure. The relative crystallinity of this compound, which is essential for comprehending how well it performs in adsorption applications, can also be inferred from the peak intensity. Prior research in the literature has reported similar results showing increased stabilization of CuMgFe-CO3 and CuMgFe-SO4 in the formation of orderly-grown primary particles, resulting in larger platelets with a sand rose morphology [8].

J. of Advanced Mechanical Engineering Applications Vol. 6 No. 1 (2025) p. 80-93

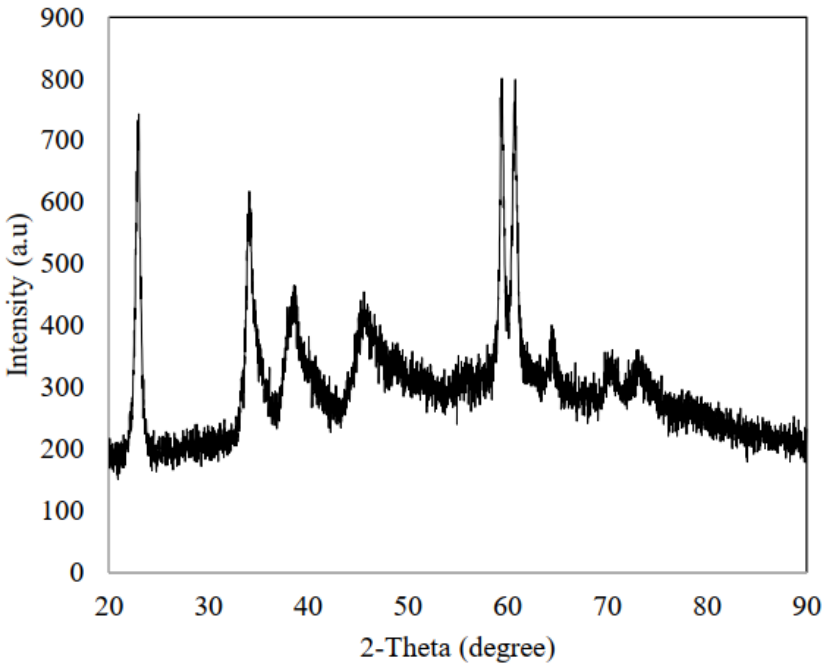

Fig. 8 *XRD graph of MgFeCu.CO3 compound*

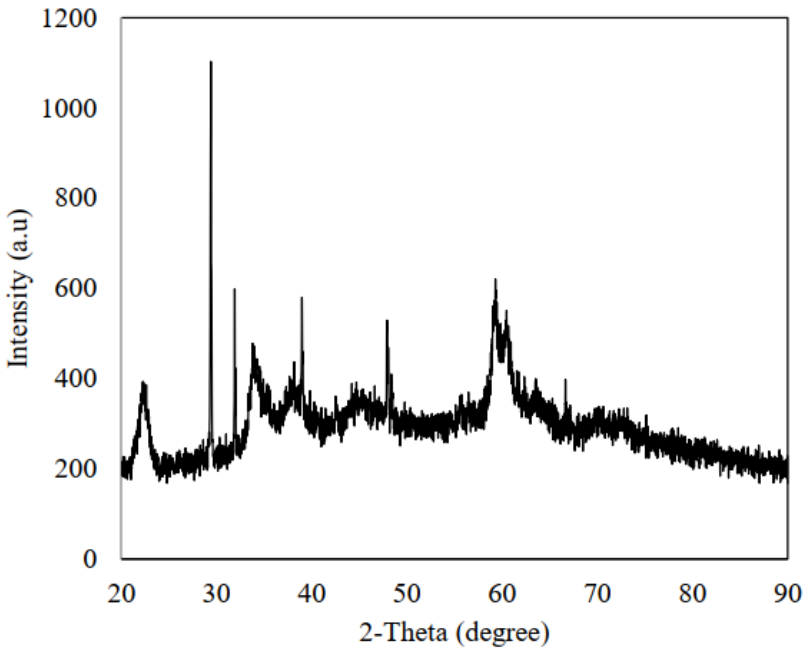

Fig. 9 *XRD graph of MgFeCu.NO3 compound*

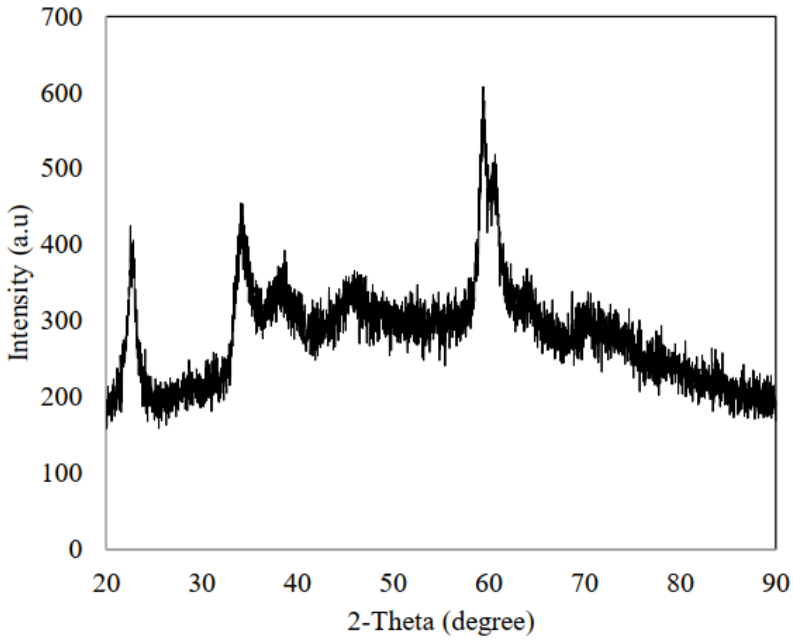

Fig. 10 *XRD graph of MgFeCu.SO4*

However, when combined with other anions such as CuMgFe-NO3, the LDH can display a morphology similar to that of a stone. The formation of this type of structure, which leads to a smaller specific area and higher platelet packing than LDHs made with CO32-, explains the observed crystallite sizes and specific area. The diffractograms for $MgFeCu.SO_4$ show that prismatic or plate-like particles are forming. Strong ionic bonds between sulfate ions and metal cations are responsible for this property, which allows for controlled growth along crystallographic axes. This compound's unique shapes indicate that specific synthesis techniques, like hydrothermal methods or slow crystallization processes, were used. Furthermore, rough surfaces or faceting—indicators of high crystallinity may arise from the growth environment being impacted by impurities or fluctuating conditions [8].

Water and anions make up the LDH interlayer, and they are connected to the hydroxide layer by H-bonding. The tendency to be intercalated is generally influenced by the electrostatic interaction between the anion and the lamellae, which increases with the anion's charge density. As a result, the ease of intercalation with the inorganic anions investigated in this work is as follows: CO32- > SO42- > NO3- in the interlamellar space of LDH [8].

3.2 Effect of Contact Time on Dye Adsorption

Table 1 shows the amount of MO adsorbed by MgFeCu-LDH as a contact time indicator from UV 1800 Shimadzu spectrophotometer. Prior to the experiment, MO had a value of 3.847. Table 2 and Fig. 11 show dye removal, R(%) of MO after experiment. The kinetic study indicates that the adsorption equilibrium is determined by the highest value. The following formula (Eq.1) is used to calculate the percentage removal (R%) of dye:

$$R(\%) = \frac{(C_0 - C_e) \times 100}{C_0} \quad (1)$$

According to the study, the amount of dye adsorbed rises with time and reaches equilibrium after a predetermined amount of time. This suggests that the adsorption process starts with fast surface adsorption and then moves more slowly toward equilibrium as the adsorbent sites fill up. The percentage removal (R%) for the Mg–Fe–LDH material varied over time and among the various anionic forms (CO3, NO3, and SO4). The results emphasize the significance of time optimization for maximum dye removal by indicating that contact time has a significant impact on adsorption efficiency.

Table 1 *Concentration (absorbance, A) of MO after experiment from UV 1800 Shimadzu spectrophotometer*

Time (min)	Concentration (Absorbance, A)		
	$MgFeCu.CO_3$	$MgFeCu.NO_3$	$MgFeCu.SO_4$
5	2.791	2.175	2.439
10	2.862	1.948	2.281
20	2.642	1.934	2.205
30	2.700	2.261	2.134
50	2.934	1.943	2.194
70	2.876	2.096	1.941
90	2.957	2.238	2.179
120	2.575	2.010	2.432
150	2.816	1.944	2.242

Table 2 *Dye removal, R (%) of MO after experiment*

Time (min)	Dye Removal, R (%)		
	$MgFeCu.CO_3$	$MgFeCu.NO_3$	$MgFeCu.SO_4$
5	27.450	43.462	36.600
10	25.604	49.363	40.707
20	31.323	49.727	42.683
30	29.815	41.227	44.528
50	23.733	49.493	42.969
70	25.240	45.516	49.545
90	23.135	41.825	43.358
120	33.065	47.751	36.782
150	26.800	49.467	41.721

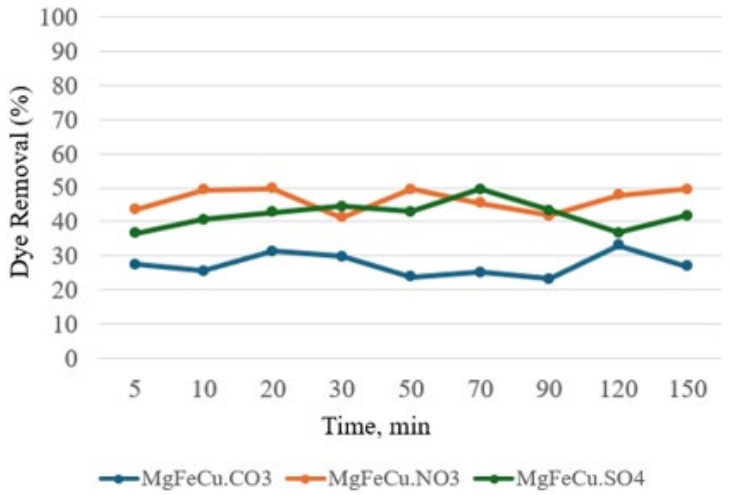

Fig. 11 *Dye removal over time graph*

3.3 Kinetic Adsorption Study

Adsorption is frequently accomplished through a chemical reaction involving the adsorbate and functional groups on the adsorbent surface. Various kinetic models have been used to explain the arrangement of interactions between the adsorbate and adsorbent. In this study, we used Lagergren's pseudo-first order model. When adsorption occurs first, followed by diffusion across a boundary, the kinetics usually follow Lagergren's pseudo-first-order equation [9]:

$$\log(q_e - q_t) = \log qe - \left(\frac{k_1}{2.303}\right)t \quad (2)$$

In the pseudo-first-order adsorption process, k1 is the rate constant (min−1), and qt and qe are the adsorbed amounts (mg/g) at time t (min) and equilibrium, respectively. The image shows that plotting log (qe - qt) versus t results in a straight line for first-order kinetics, allowing for the computation of the adsorption rate constant, k1. Table 3 and Fig. 12 show the computed parameters for the pseudo-first-order kinetic model. The estimated qe (mg/g) value for the dye under investigation differs from the experimental value. This shows that the pseudo-first-order kinetic model [10] cannot effectively represent adsorption kinetics.

Table 3 *First order kinetic model for adsorption of MO onto Mg–Fe–LDH*

Time (min)	MgFeCu.CO3 ln(qe−qt)	MgFeCu.NO3 ln(qe−qt)	MgFeCu.SO4 ln(qe−qt)
5	-0.887	-0.840	-0.524
10	-0.764	-2.076	-0.690
20	-1.396	-∞	-0.799
30	-1.125	-0.707	-0.935
50	-0.667	-2.268	-0.818
70	-0.743	-1.012	-∞
90	-0.640	-0.739	-0.844
120	-∞	-1.341	-0.530
150	-0.840	-2.222	-0.742

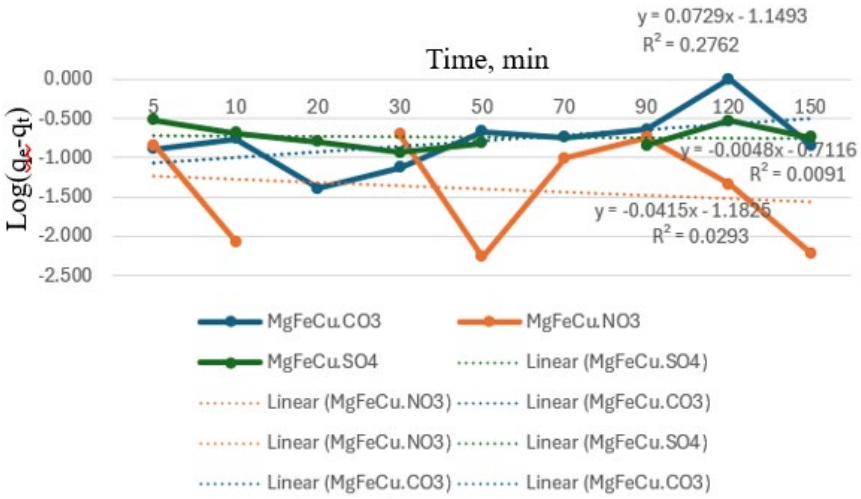

Fig. 12 *First order kinetic model for adsorption of MO onto MgFeCu-LDH graph*

According to a number of writers, in some cases, these interactions can be characterized using second-order kinetics. The pseudo second-order kinetic equation is expressed as [11]:

$$\frac{t}{q_t} = \frac{1}{k_2 q_e^2} + \left(\frac{1}{q_e}\right)t \quad (3)$$

Where k2 (g mg−1 min−1) represents the second-order rate constant. Table 4 and plots of t/qt vs. t displayed in Fig. 13 allow for the derivation of qe and k2 parameters to assess second-order kinetics. The correlation coefficient (R2) displays a strong link between the parameters and demonstrates that MO sorption is pseudo-second-order kinetics. The relationship is linear. Table 5 shows that, in comparison to the value of the pseudo-first order kinetic model, the correlation coefficient (R2) for the pseudo-second order kinetic model is extremely

high, approaching unity. The experimental results and the calculated equilibrium sorption capacity (qe) accord. These findings confirm that the pseudo-second-order sorption mechanism is dominant, and that a chemisorption process appears to modulate the sorption process's overall rate constant [12]:

Table 4 *Second order kinetic model for adsorption of MO onto Mg–Fe–LDH*

Time (min)	MgFeCu.CO3 t/qt	MgFeCu.NO3 t/qt	MgFeCu.SO4 t/qt
5	7.891	4.984	5.919
10	16.920	8.777	10.643
20	27.663	17.425	20.300
30	43.592	31.526	29.189
50	91.274	43.768	50.413
70	120.151	66.629	61.210
90	168.539	93.226	89.928
120	157.233	108.873	141.343
150	242.483	131.372	155.763

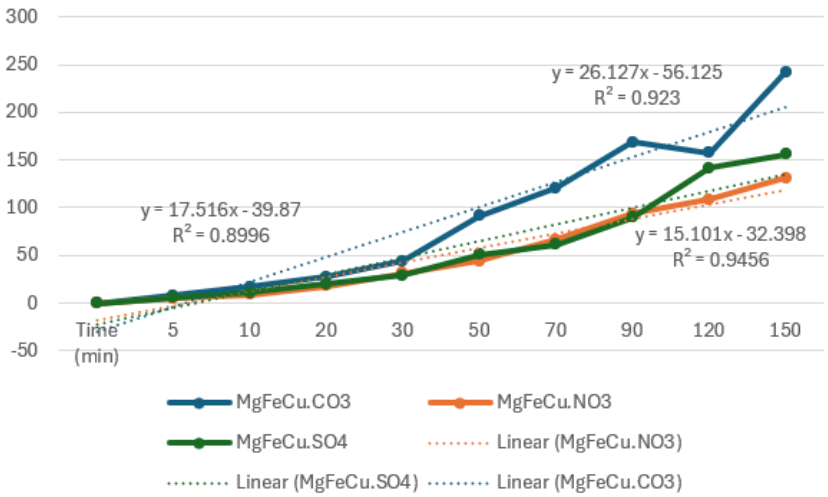

Fig. 13 *Second order kinetic model for adsorption of MO onto MgFeCu-LDH graph*

Table 5 *Data collected from the graph first and second order*

	First-order parameter		Second-order parameter	
	K_1 (min^{-1})	R^2	K_2 (g/mg min)	R^2
$MgFeCu.CO_3$	0.0729	0.2762	1464.9	0.923
$MgFeCu.NO_3$	0.0415	0.0293	489.2	0.9456
$MgFeCu.SO_4$	0.0048	0.0091	698.9	0.8996

The following formula can be used to assess how intraparticle diffusion resistance affects adsorption:

$$q = k_i t^{1/2} + C \tag{4}$$

where ki represents the intraparticle diffusion rate constant (mg g–1 min–0.5). The values of C show the thickness of the boundary layer. The qt vs. t1/2 charts in Fig. 14 resulted in straight lines. The regression coefficient and rat constant for intra-particle diffusion (ki) are shown in the table below. The linearity of the graphs revealed that intraparticle diffusion could have a considerable influence on the MO dye's adsorption onto LDH material. The process by which the dye was deposited on LDH material could not be explained by a simple surface-only mechanism; rather, adsorption on the external surface was followed by diffusion into the pores as

well as various surface kinks and steps [13].

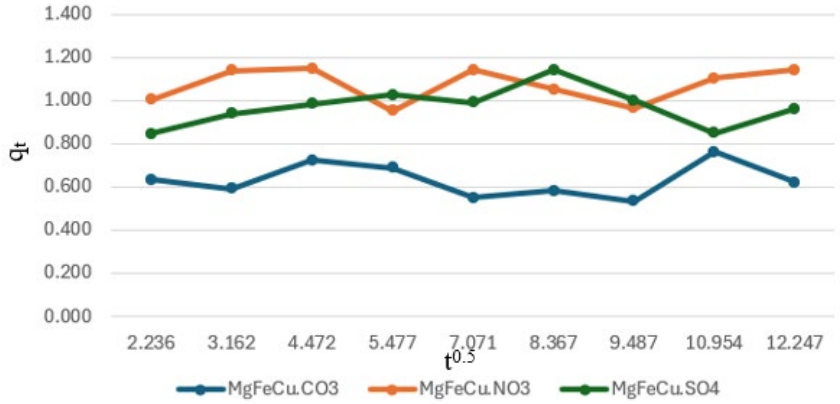

Fig. 14 *Intraparticle diffusion kinetic for adsorption of MO onto MgFeCu-LDH*

The pseudo-second-order model more closely matches the experimental data than the pseudo-first-order model, per the kinetic analysis. The pseudo-second-order model's higher correlation coefficients (R2) imply that chemisorption, which involves the adsorbate and adsorbent exchanging or sharing electrons, primarily controls the adsorption process [12]. The t/qt versus t plots' linear relationship lends more credence to this.

Furthermore, the intraparticle diffusion model shows that both surface adsorption and diffusion inside the adsorbent pores affect adsorption. These results are consistent with earlier studies that show pseudo-second-order kinetics to be a good predictor for systems in which chemisorption is an important part of the adsorption process [9].

4. Conclusion & Recommendations

In conclusion, the study found that incorporating different interlamellar anions (CO_3^{2-}, NO_3^-, and SO_4^{2-}) resulted in significant structural and functional differences that affected the adsorption efficiency. These materials may be helpful precursors to MgFeCU-LDHs intercalated with a range of inorganic anions for use in the adsorption of anionic reactive dye from aqueous solution (it is an effective positively charged adsorbent) as the interlayer chloride ions may be readily replaced by carbonate ions. FESEM and XRD were used to characterize the produced LDH.

Overall, the findings demonstrate that Mg–Fe–Cu.NO_3–LDH is especially effective at eliminating MO. After 20 minutes, the adsorption of MO on Mg–Fe–Cu-NO_3–LDH reached equilibrium for the removal of 100 mg/L CR. The pseudo second order was fitted to the adsorption data. For Mg–Fe–Cu-NO_3–LDH, the maximum removal and highest MO adsorbed is 49.727. The research findings result in several important recommendations suggested to enhance the wastewater treatment and direct further research. Doping LDHs with photocatalytic materials, like TiO_2, to improve their capacity to break down dyes when exposed to light is another interesting strategy. To fully utilize LDHs' potential for effective dye removal in wastewater treatment, more investigation into the synthesis parameters and catalytic mechanisms is necessary.

Several crucial elements must be improved in order to enhance the experimental outcomes for the use of LDHs as catalysts for the treatment of dye wastewater. To find the best metal ions for dye degradation, the metal composition of the LDHs should first be adjusted. Finding the metals with the highest catalytic efficiency can be aided by testing other metal combinations, such as Fe-Al, Cu-Al, and Zn-Al. Finding the ideal balance that improves catalytic efficiency also requires methodically examining other metal ratios, such as the Mg/Al ratio, or investigating different combinations, such as Fe-Zn. Second, the synthesis process should be modified to enhance the LDHs' shape, especially by raising porosity to optimize the surface area available for dye adsorption. To create more porous or sheet-like LDHs, controlled synthesis parameters including temperature, pH, and reaction time should be adjusted. This might improve the adsorption capacity and catalytic [14][15]. These recommendations seek to raise the quality of adsorption by the catalyst, direct future research, and increase the efficiency of wastewater treatment process.

Acknowledgement

The authors acknowledge the support from Universiti Tun Hussein Onn Malaysia throughout this project.

Conflict of Interest

Authors declare that there is no conflict of interests regarding the publication of the paper.

Author Contribution

The authors confirm contribution to the paper as follows: ***study conception and design:*** *Muhamad Syaza bin Mohd Sahabudin, Norrizal Bin Mustaffa, Nurasyikin Binti Misdan;* ***data collection:*** *Muhamad Syaza bin Mohd Sahabudin, Nurasyikin Binti Misdan;* ***analysis and interpretation of results:*** *Muhamad Syaza bin Mohd Sahabudin, Nurasyikin Binti Misdan;* ***draft manuscript preparation:*** *Muhamad Syaza bin Mohd Sahabudin, Nurasyikin Binti Misdan. All authors reviewed the results and approved the final version of the manuscript.*

References

[1] Amit Sonune, & Rupali Ghate. (2004, August). *Developments in Wastewater Treatment Methods*. ResearchGate; Elsevier BV. https://www.researchgate.net/publication/228905514_Developments_in_Wastewater_Treatment_Methods

[2] Fu, Y., Fu, X., Song, W., Li, Y., Li, X., & Yan, L. (2023). *Recent progress of layered double Hydroxide-Based materials in wastewater treatment. Materials*, 16(16),5723. https://doi.org/10.3390/ma16165723

[3] Yang, D., Chen, Y., Li, J., Li, Y., Song, W., Li, X., & Yan, L. (2022). Synthesis of calcium–aluminum-layered double hydroxide and a polypyrrole decorated product for efficient removal of high concentrations of aqueous hexavalent chromium. *Journal of Colloid and Interface Science*, *607*, 1963–1972. https://doi.org/10.1016/j.jcis.2021.10.014

[4] Xie, Z.-H., Zhou, H.-Y., He, C., & Lai, B. (2021). *Synthesis, application and catalytic performance of layered double hydroxide based catalysts in advanced oxidation processes for wastewater decontamination: A review.* ResearchGate; Elsevier BV. https://www.researchgate.net/publication/349083141_Synthesis_application_and_catalytic_performance_of_layered_double_hydroxide_based_catalysts_in_advanced_oxidation_processes_for_wastewater_decontamination_A_review

[5] Maria, B., Rangabhashiyam S, Giannakoudakis, D. A., & Meili, L. (2022). *Layered Double Hydroxides as Rising-Star Adsorbents for Water Purification: A Brief Discussion*. ResearchGate; MDPI. https://www.researchgate.net/publication/362373864_Layered_Double_Hydroxides_as_RisingStar_Adsorbents_for_Water_Purification_A_Brief_Discussion

[6] Fan, G., Li, F., Evans, D. G., & Duan, X. (2014). Catalytic applications of layered double hydroxides: recent advances and perspectives. *Chemical Society Reviews*, *43*(20), 7040–7066. https://doi.org/10.1039/c4cs00160e

[7] Kute, M. (2018). *Adsorption of methylene blue using Ni/Fe layered double hydroxide*. ResearchGate; unknown. https://www.researchgate.net/publication/338139682_Adsorption_of_methylene_blue_using_NiFe_layered_double_hydroxide

[8] De, N., Lima, G., Ramirez-Ubillus, M. A., Li, C., Hammer, P., Serge Chiron, & Pupo, R. F. (2022). Effect of the interlamellar anion on CuMgFe-LDH in solar photo-Fenton and Fenton-like degradation of the anticancer drug 5-fluorouracil. *Applied Catalysis. B, Environmental*, *315*, 121537–121537. https://doi.org/10.1016/j.apcatb.2022.121537

[9] Ahmed, I.M. and Gasser, M.S. (2012) *Adsorption Study of Anionic Reactive Dye from Aqueous Solution to Mg-Fe- CO3 Layered Double Hydroxide (LDH). Applied Surface Science, 259, 650-656. - References - Scientific Research Publishing.* (2015).

[10] Ni, Z.-M., Xia, S.-J., Wang, L.-G., Xing, F.-F., & Pan, G.-X. (2007). Treatment of methyl orange by calcined layered double hydroxides in aqueous solution: Adsorption property and kinetic studies. *Journal of Colloid and Interface Science*, *316*(2), 284–291. https://doi.org/10.1016/j.jcis.2007.07.045

[11] Ridha Lafi, Khaled Charradi, Mohamed Amine Djebbi, Haj, B., & Amor Hafiane. (2016). Adsorption study of Congo red dye from aqueous solution to Mg–Al–layered double hydroxide. *Advanced Powder Technology*, *27*(1), 232–237. https://doi.org/10.1016/j.apt.2015.12.004

[12] Villar, M., Rangabhashiyam Selvasembian, Giannakoudakis, D. A., Triantafyllidis, K. S., McKay, G., & Meili, L. (2022). Layered Double Hydroxides as Rising-Star Adsorbents for Water Purification: A Brief Discussion. *Molecules/Molecules Online/Molecules Annual*, *27*(15), 4900–4900. https://doi.org/10.3390/molecules27154900

[13] Xie, Z.-H., Zhou, H.-Y., He, C., & Lai, B. (2021, February). *Synthesis, application and catalytic performance of layered double hydroxide based catalysts in advanced oxidation processes for wastewater decontamination: A review.* ResearchGate; Elsevier

[14] Yang, Z., Wang, F., Zhang, C., Zeng, G., Tan, X., Yu, Z., Zhong, Y., Wang, H., & Cui, F. (2016). *Utilization of LDH-based materials as potential adsorbents and photocatalysts for the decontamination of dyes wastewater*: a review. RSC Advances, 6(83), 79415–79436. https://doi.org/10.1039/c6ra12727d

[15] Yang, D., Chen, Y., Li, J., Li, Y., Song, W., Li, X., & Yan, L. (2022). Synthesis of calcium–aluminum-layered double hydroxide and a polypyrrole decorated product for efficient removal of high concentrations of aqueous hexavalent chromium. *Journal of Colloid and Interface Science*, *607*, 1963–1972. https://doi.org/10.1016/j.jcis.2021.10.014

[16] Cano, L. A., Barrera, D., Villarroel-Rocha, J., & Sapag, K. (2023). Influence of the synthesis method of layered double hydroxides on the textural properties and nitrate removal. *Catalysis Today*, *422*, 114222. https://doi.org/10.1016/j.cattod.2023.114222